Experimental Thermal and Fluid Science 168 (2025) 111501

Contents lists available at ScienceDirect

Experimental Thermal and Fluid Science

journal homepage: www.elsevier.com/locate/etfs

Phase identification of single microdroplet impacting a hot surface

Michael Hennessy, Mahsa Ebrahim *

Loyola Marymount University, 1 LMU Dr., Los Angeles, CA, 90045, USA

ARTICLE INFO

Keywords:
Microdroplet
Spray cooling
Phase diagram
Droplet lifetime

ABSTRACT

Fundamental understanding of the physics of droplet impingement is essential in order to design an efficient spray cooling system. While there is extensive literature on single macrodroplet impingement, the results do not apply to spray cooling since the droplets in a spray are microscopic. In the present study, the impact of single microdroplets on a heated surface was experimentally investigated for a broad range of liquids, impact Re and We numbers, and for $60 < T < 250°C$. It was found that the heat transfer regimes were independent of the impact velocity. A properly scaled phase diagram was developed to identify the heat transfer regime of a microdroplet's impact given the impact conditions. An analytical model was proposed using the conservation laws to estimate the droplet lifetime on the hot surface in the film evaporation regime.

1. Introduction

Spray cooling is known as one of the most promising cooling techniques for high heat flux electronics. To understand the complex physics of spray cooling, improve it, and promote its application in electronics, many researchers have focused on studying single droplet impingement to investigate its fundamentals at the scale of a single droplet. There are comprehensive reviews on state-of-the-art research and the rich literature on macrodroplet impingement on dry unheated surfaces, heated surfaces covering all heat transfer regimes, and wet surfaces with and without heat transfer [1–3]. As such, only some of the more relevant work is reviewed here to highlight the gaps in the literature and the importance of this study.

Most researchers only considered the We number to capture the characteristic parameters involved in droplet impingement dynamics [1,2,4–6]. For example, correlations have been developed to predict the maximum dimensionless spreading factor, D_{max}/D as a function of the impact We number [4,5]. Researchers have developed phase diagrams for the impact of macroscopic droplets on a heated surface where only the We number was used to normalize the data [4,7,8]. However, it has been shown that the We number cannot sufficiently capture all influential parameters involved in impact dynamics [1,2,9,10]. For example, numerical simulations have revealed that the Re number independently affects the droplet spreading phase after the impact [9,10]. Furthermore, current regime maps for the same heat transfer regime differ for different liquids and cannot be applied to the same liquid but different size scale [1,2,7,8,11]. It may be possible to match the We number of macroscopic and microscopic droplets by adjusting their impact velocities, their Re number will be orders of magnitude different and therefore, the physics at play will differ. While much can be learned from the rich literature of the heat transfer of a single macrodroplet impacting a heated surface, the results are fundamentally different from those of microdroplets and hence inapplicable to spray cooling.

Although macrodroplets have been extensively studied [1–3], only few studies have been conducted on the impact of a single microdroplet due to the complexity of generating single microdroplets and instrumentation at that scale [2]. Visser et al. studied microdroplet impacts for velocities up to 100 $\frac{m}{s}$ on an unheated surface [12]. They concluded that to use the existing models for macrodroplets for microdroplets, such as the model developed by Pasandideh-Fard et al. [13], a 180° angle should be used as the initial contact angle. They also showed that the dimensionless boundary layer thickness was proportional to $D\mathrm{Re}^{-1/2}(\frac{tV}{D})^{0.45}$. Ko and Chung [14] studied the effects of impact velocity, impinging angle, and droplet diameter on the breakup probability of n-decane microdroplets in the Leidenfrost regime. A nonlinear relation was observed between the surface temperature and the break up possibility. Kim et al. [15] visualized the hydrodynamics of a microdroplet impacting a dry unheated surface. They observed similar trends in the spreading factor as in previous work for macrodroplets, i.e., microdroplets at higher impact velocities spread more. Hu and Liu [16] numerically modeled a microdroplet impacting on an unheated superhydrophobic surface using volume-of-fluid (VOF) method. They concluded that the effect of Laplace pressure was not negligible due to the small size of the droplet.

In addition to single microdroplets, one or multiple streams of periodic microdroplets at high frequencies on a heated surface have been investigated by a few researchers [17–21]. Zhang et al. [17]

* Corresponding author.
E-mail address: mahsa.ebrahim@lmu.edu (M. Ebrahim).

https://doi.org/10.1016/j.expthermflusci.2025.111501
Received 13 December 2024; Received in revised form 6 March 2025; Accepted 17 April 2025
Available online 29 April 2025

Nomenclature

A_c	Contact area, m^2
A_s	Surface area, m^2
D_{AB}	Mass diffusivity, $\frac{m^2}{s}$
C_p	Specific heat, $\frac{J}{kg\ K}$
h_{fg}	Enthalpy of vaporization, $\frac{J}{kg}$
D	Droplet initial diameter, m
Ec	Eckert number, Ec = $\frac{V^2}{C_p \Delta T}$
h	Heat transfer coefficient, $\frac{W}{m^2\ K}$
Ja	Jacob number, Ja = $\frac{C_p \Delta T}{h_{fg}}$
k	Thermal conductivity, $\frac{W}{m\ K}$
l	Droplet height on the surface, m
M	Molar mass, $\frac{kg}{mol}$
m	Droplet mass, Kg
N	Molar flux, $\frac{mol}{m^2\ s}$
Oh	Ohnesorge number, Oh = $\frac{\mu}{\sqrt{\rho \sigma D}}$
P	Pressure, Pa
q	Heat flow, W
q"	Heat flux, $\frac{W}{m^2}$
R	Contact radius, m
r	Radial direction
Re	Reynolds number, Re = $\frac{\rho D V}{\mu}$
T	Temperature, °C
t	Time, s
V	Droplet impact velocity, $\frac{m}{s}$
We	Weber number, We = $\frac{\rho D V^2}{\sigma}$
x	Molar fraction

Greek symbols

Π	Dimensionless number, $\Pi = \frac{Ja^2}{Oh}$
α	Thermal diffusivity, $\frac{m^2}{s}$
β	Contact angle, °
μ	Dynamic viscosity, Pa s
ρ	Density, $\frac{kg}{m^3}$
σ	Surface tension, $\frac{N}{m}$
τ	Dimensionless time, $\tau = \frac{t\alpha}{D^2}$
θ	Dimensionless temperature, $\theta = \frac{T_s - T_\infty}{T_{sat} - T_\infty}$

Subscripts

∞	Ambient
conv.	Convection
evap.	Evaporation
in	Input
s	Surface
sat	Saturation
$\tilde{t}$	Time constant, s

identified an optimum spacing between microdroplets to reduce the collision and splashing to enhance heat transfer. Soriano et al. [18] observed that the spacing between adjacent droplet streams played a key role in film dynamics, and convection was most effective when the radial velocity in the liquid film was maximized. Dunand et al. [19] showed that the droplet size highly affected the contribution of sensible heat gained by the droplet to the wall cooling. Sellers and Black [20] found that the critical heat flux values for a periodic microdroplet impact were roughly twice the heat flux for traditional pool boiling for the same super heated surface. An optimal frequency was identified by Chou et al. [21] at which the temperature of the hot microspot was maintained constant during the impact of periodic microdroplets.

Despite the motivation behind droplet impingement studies being an enhancement in spray cooling, the current state-of-the-art in this field is inapplicable to spray cooling and lacks the fundamental understanding of heat transfer in micro scale. Although spray cooling is much more complicated than single droplet impingement, spray cooling can benefit from fundamental knowledge of microdroplets, such as a phase diagram at the right scale. For instance, a phase diagram can assist in modulating the spray conditions to expect a desired heat transfer regime depending on the surface temperature.

This paper experimentally investigates the impact of single microdroplets on a heated surface for surface temperatures ranging from below saturation to above the Leidenfrost regime for $0.1 \leq We \leq 6.5$ and $2 \leq Re \leq 75$. A piezoelectric micro dispenser was used to generate single microdroplets. Three different liquids (ethanol, isobutanol, and isopropanol) were used to study the thermo-physical properties of liquids on the heat transfer regimes. A high-speed digital video camera equipped with a microscopic lens was utilized to observe the droplet dynamics after the impact as well as measuring the droplet lifetime on the surface. An appropriately normalized phase diagram was developed for the impact of a microdroplet on a heated surface. An analytical model was developed for the lifetime of a microdroplet in the film evaporation regime ($T < T_{sat}$).

2. Experimental apparatus

The schematics of different parts of the experimental apparatus designed to generate single microdroplets and investigate their dynamics on a heated surface are shown in Fig. 1. The experimental apparatus consists of (i) the piezoelectric dispenser, (ii) the pressure controller, (iii) the heated surface, and (iv) dynamic visualization. The details of each part are as follows.

(i) Piezoelectric dispenser- A MicroFab piezoelectric dispenser with varying orifice diameters (90 and 120 μm) was utilized to generate single microdroplets. The dispenser contains a glass capillary tube that is encapsulated inside an annular radially poled piezoelectric tube was connected to the fluid reservoir (a syringe), as seen in Fig. 1. A unipolar trapezoidal voltage wave, shown in Fig. 2, was used to excite the piezo tube and generate microdroplets [22]. MicroFab JetDrive V was used with MicroFab JetServer software as the function generator to finely control the wave shape parameters (rise, fall, dwell times, and amplitude). Each liquid's wave shape was adjusted depending on its surface tension and viscosity. Furthermore, different amplitude and dwell times were tried for each liquid to vary the droplet diameter and velocity.

(ii) Pressure controller- The piezoelectric dispenser requires intricate pressure control to maintain the liquid flush at the dispenser's orifice before excitation. Thus, the pressure inside the liquid reservoir was a key parameter in generating microdroplets. A vacuum chamber up to −750 mmHg was created using a Huanyu Diaphragm Vacuum Pump. A MicroFab pressure regulator was utilized to control the reservoir's pressure. The reservoir pressure was separately adjusted for each liquid depending on its surface tension. Less than −14 mmHG of vacuum pressure was required for all liquids tested in this paper.

(iii) Heated surface- A 3.5″ copper rod of 1″ in diameter at the top and 1.5″ diameter at the bottom, with three inserted cartridge heaters (2″ length, 30 W, and 3/16″ diameter) from the bottom, was used to make the heated target surface. The target surface end of the copper rod was CNC machined and polished to reduce the roughness. The surface roughness was not measured; however, based on a similar sample, the roughness is expected to be ≈3 μm. A contact angle of approximately 35° at T_∞ was measured on the target surface for the three liquids studied. Five type K thermocouples were inserted from the side close to the top of the rod to monitor surface temperature and measure the

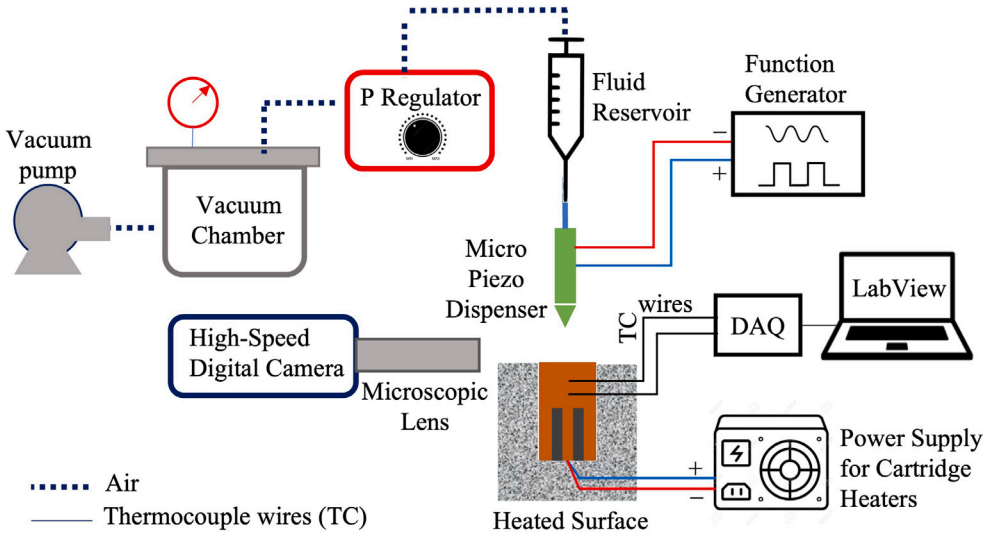

Fig. 1. Schematic of the experimental apparatus.

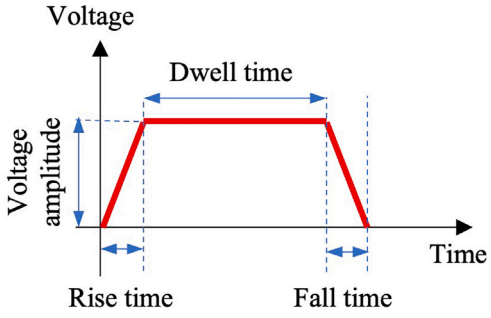

Fig. 2. Unipolar trapezoidal voltage wave.

Table 1
Thermophysical properties of tested liquids at 20 °C and 1 atm.

	Cp [$\frac{kJ}{kg\ K}$]	σ [$\frac{mN}{m}$]	μ [cPa s]	ρ [$\frac{kg}{m^3}$]	T_{sat} [°C]
Ethanol	2.46	22	1.2	789	78
Isobutanol	2.27	23	3.9	802	107.9
Isopropanol	2.56	21.8	2.1	786	82.6

Table 2
Variation of tested impact conditions.

	D [°C]	V [$\frac{mm}{s}$]	Re	We	T_s [C]
Min.	25 ± 3.2	150 ± 3.5	2	0.01	60 ± 2.9
Max.	75 ± 2.4	1600 ± 78	75	6.5	250 ± 4.3

heat flux using data acquisition (DAQ-9133 and NI 9211) and LabView. The heater was carefully insulated on the side and the bottom with a ceramic fiber blanket 3023E and placed inside a wooden box.

(iv) Dynamic visualization- Droplet generation and impact dynamics were closely observed using a high-speed digital camera (Phantom Vision Research V711) and microscopic lens (Infinity, Model K2 DistaMax). LED lights (GS Vitec, MultiLed QT) were utilized to provide sufficient illumination. Videos were recorded at 30,000 fps with a resolution of 320 by 320 pixels. Microdroplet initial diameter and velocity and its lifetime on the surface were measured by frame-by-frame analysis in the Phantom Camera Control (PCC) software.

3. Results and discussion

Three liquids of Ethanol, Isopropanol, and Isobutanol were used to generate microdroplets. The thermophysical properties of these liquids are shown in Table 1. The variation of impact condition is listed in Table 2. As mentioned before, the impact velocity and initial diameter, and droplet lifetime (contact time on the surface or the duration to full evaporation) were measured using the frame by frame analysis of high-speed videos. For each surface temperature, each impact condition was repeated five to eight times and ensemble averaged. The surface temperature was only recorded and reported before the impact as the surface temperature was assumed not to be influenced by the microdroplet (due to the negligible size of droplets compared to the surface). Thus, the effects of thermophysical properties of the solid surface were not studied in this research. Uncertainties were calculated as two times the standard deviation of the repeated measurements. Since numerous data points were collected, only a few examples of the uncertainty in the measured data (indicated as error bars) are shown for ethanol in Fig. 3. The choice for nondimensionalizing the lifetime in Fig. 3(b) is explained in Section 3.2. The uncertainty in τ is calculated using the propagation of uncertainty method using the uncertainties of the diameter and the lifetime.

3.1. Phase diagram

Four distinct heat transfer regimes of film evaporation, nucleation boiling, transitional boiling, and film boiling or Leidenfrost were identified for microdroplet impingement on a heated surface. As an example, time elapsed images and the distinct heat transfer regimes of ethanol microdroplets are shown in Fig. 4. As expected, as the surface temperature increases, the evaporation rate increases until the surface reaches the critical heat flux.

To date, phase diagrams or regime maps showing different droplet impact outcomes are illustrated using the impact We number and surface temperature. An example of such a phase diagram from Staat et al. [23] is shown in Fig. 5. Similar phase diagrams can be found in [4,24–26]. However, all these diagrams were developed for macroscale droplets and used the We number for scaling. Roisman et al. [27] and Ebrahim et al. [9] showed that using only the We number to classify the impact outcomes is incorrect since the We number does not capture any thermophysical properties of the liquid. Furthermore, it was shown by Ebrahim et al. [9] that the Re number can independently affect the impact dynamics, making the droplet impact a multi-dimensionless group problem. Since matching both We and Re numbers is impossible for macro- and microscopic droplets, the phase diagrams developed for macrodroplets cannot be applied to microdroplets. To further demonstrate these differences, the results of this

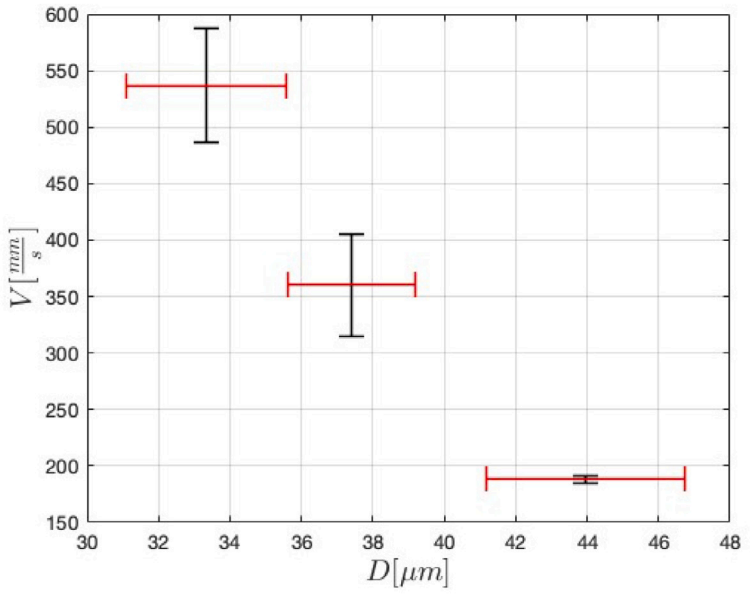

(a) Impact velocity vs initial diameter

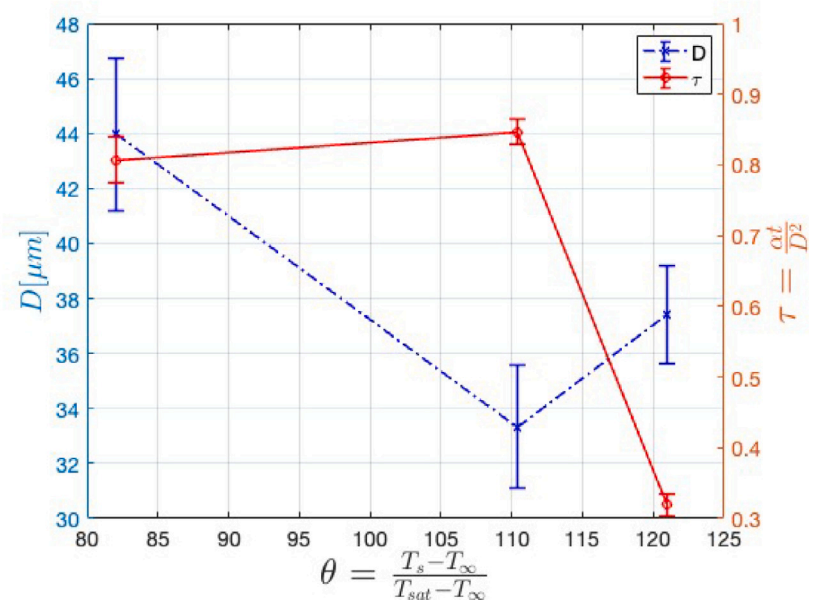

(b) Initial diameter and dimensionless lifetime vs surface temperature

Fig. 3. Examples of uncertainty of the experimental data for ethanol microdroplets.

study are first shown in a similar way to other existing phase diagrams in Fig. 6, where the ensemble-averaged data of all three liquids and all impact conditions are shown. A comparison between Figs. 5 and 6 highlights the difference between the order of magnitude of the We number and the impact regimes for macro- and microdroplets.

Furthermore, it can be speculated from Fig. 6 that as the We number increases, the onset of the Leidenfrost regime is slightly delayed, as boiling still occurs at higher temperatures. However, in the following sections, we show that impact velocity does not affect the heat transfer regimes at all. While Fig. 6 can be used as a phase diagram for microdroplet impact, it does not incorporate the effects of liquid properties such as specific heat. To properly scale the data, the Buckingham Pi theorem was applied to identify the involving dimensionless groups. The following variables were considered to affect the heat flux as follows

$$q\varepsilon = f(C_p, \rho, \mu, \sigma, \Delta T, V, D, h_{fg}) \tag{1}$$

Considering V, D, ρ, and ΔT as repeating variables, the results of the dimensionless analysis can be expressed as

$$\frac{q''}{\rho V^3} = f\left(\frac{Cp\Delta T}{V^2}, \frac{\mu}{\rho V D}, \frac{\sigma}{\rho V^2 D}, \frac{h_{fg}}{V^2}\right) \tag{2}$$

Eq. (2) can be written using the well known dimensionless groups as follows

$$\frac{q''}{\rho V^3} == f\left(\frac{1}{\mathrm{Re}}, \frac{1}{\mathrm{We}}, \mathrm{Ja}\right) \tag{3}$$

where $\mathrm{Ja} = \frac{1}{\mathrm{Ec}} * \frac{h_{fg}}{V^2} = \frac{Cp\Delta T}{h_{fg}}$ and $\mathrm{Ec} = \frac{V^2}{Cp*\Delta T}$.

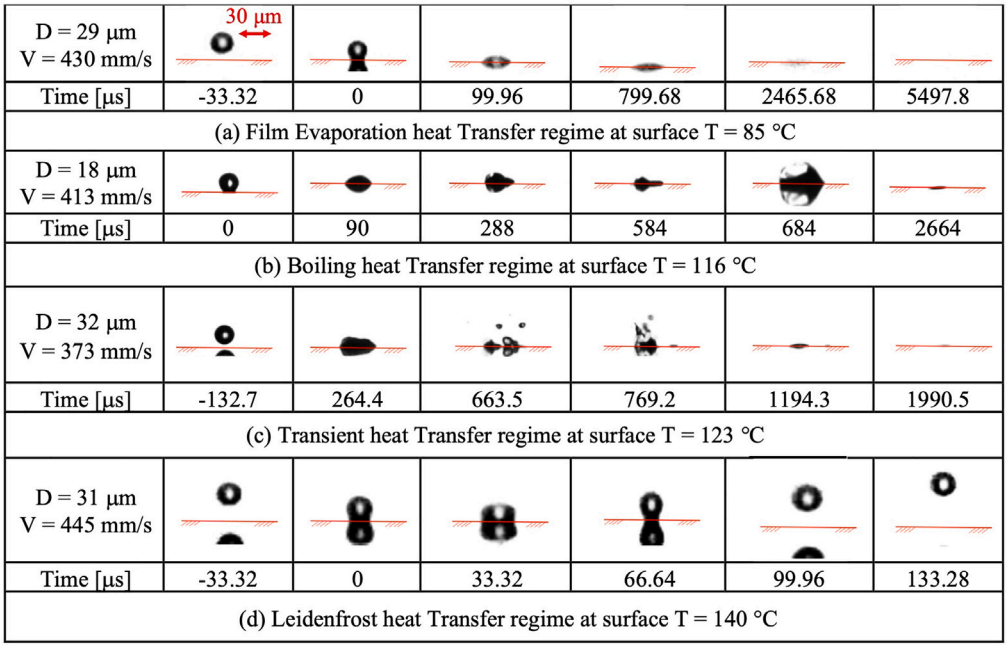

Fig. 4. Time elapsed images of the impact of an ethanol microdroplet at different surface temperatures, illustrating the four distinct heat transfer regimes.

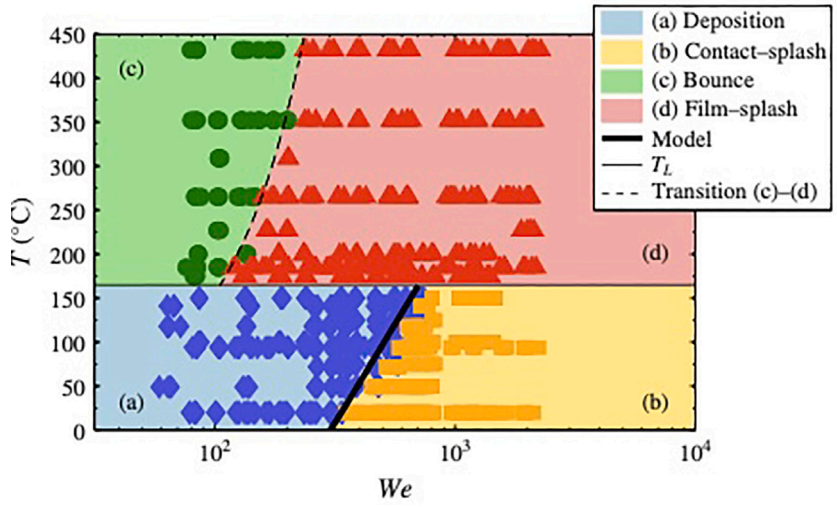

Fig. 5. Example of a phase diagram for ethanol droplets of 2.5 mm diameter impacting a sapphire plate from Staat et al. [23]. Four regimes of deposition, bounce, contact-splash, and film-splash were identified.

Finally, $\Pi = \frac{\mathrm{Ja}^2}{\mathrm{Oh}}$ was empirically chosen to scale the phase diagram where $\mathrm{Oh} = \frac{\sqrt{\mathrm{We}}}{\mathrm{Re}} = \frac{\mu}{\sqrt{\rho\sigma D}}$. All experimental data for different impact conditions (different diameters, velocities, and surface temperatures) for three liquids (ethanol, isobutanol, and isopropanol) are combined and scaled using the proposed dimensionless number, Π, in Fig. 7. Although different regimes are not perfectly divided, a dominant phase can still be identified given the impact conditions of θ and Π. It can be seen that the onset of boiling can be expected around $\Pi \approx 1.4$. The heat removal will be maximized for $1.6 \leq \Pi \leq 2.8$, and the critical heat flux can be expected for $2.6 \leq \Pi \leq 3.3$. Since both Ja and Oh numbers are independent of impact velocity, it can be concluded that the impact velocity does not affect the heat transfer regimes for the range of parameters studied in this paper.

To the best of our knowledge, the only other phase diagram appropriately scaled to capture the liquid properties was developed by Roisman et al. [27], but for macroscopic droplets. Their proposed dimensionless number included the impact velocity because, unlike a microdroplet, the kinetic energy of a macro-droplet is not negligible.

The normalized experimental data were curve fitted in MATLAB, as shown in Fig. 8. A curve fit correlation given in Eq. (4) is reasonably accurate to predict the impact parameters required to achieve a desired heat transfer regime.

$$\theta = \frac{T - T_\infty}{T_{sat} - T_\infty} = 1.103\Pi^{0.478} = 1.103\left(\frac{\mathrm{Ja}^2\mathrm{Re}}{\sqrt{\mathrm{We}}}\right)^{0.478} \quad (4)$$

The spray cooling technology can certainly benefit from the appropriately scaled phase diagram of this study (Fig. 7) and Eq. (4). For instance, for a given surface temperature, spray characteristics (droplet diameter and velocity) or the liquid can be chosen to keep $1.6 \leq \Pi \leq 2.8$ to maximize heat removal by reinforcing the boiling heat transfer regime.

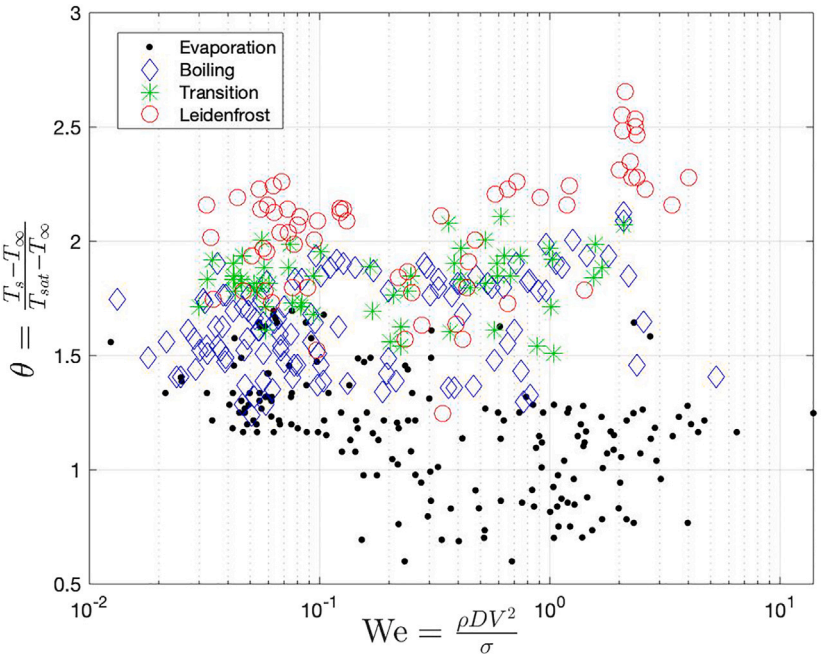

Fig. 6. Nondimensional surface temperature vs. We number. The data for all three liquids are combined and shown.

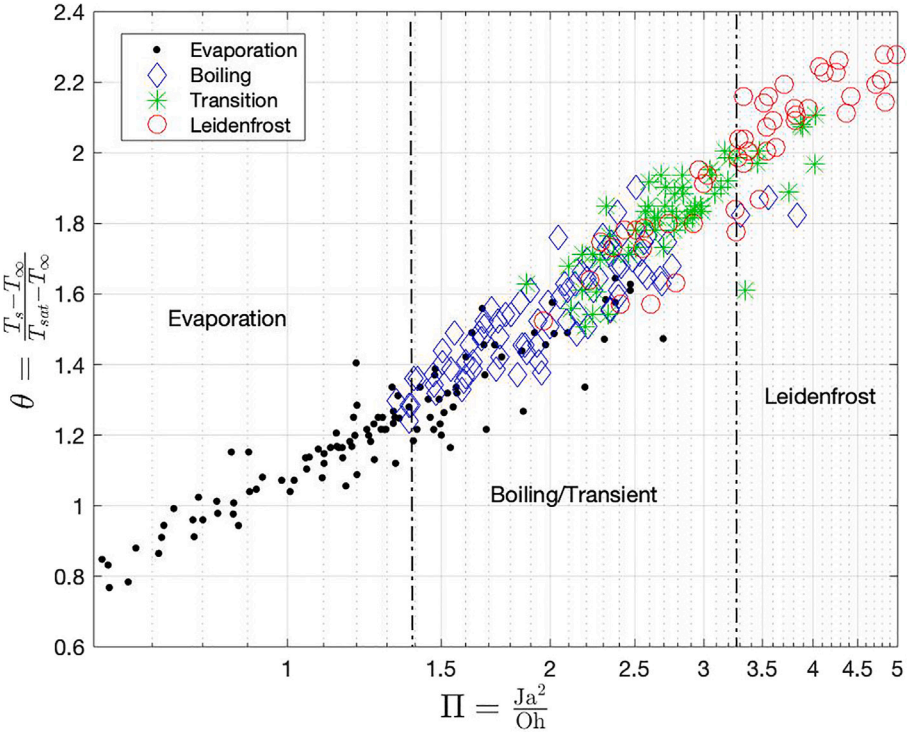

Fig. 7. Nondimensional surface temperature vs. Π number. The data for all three liquids are combined and shown.

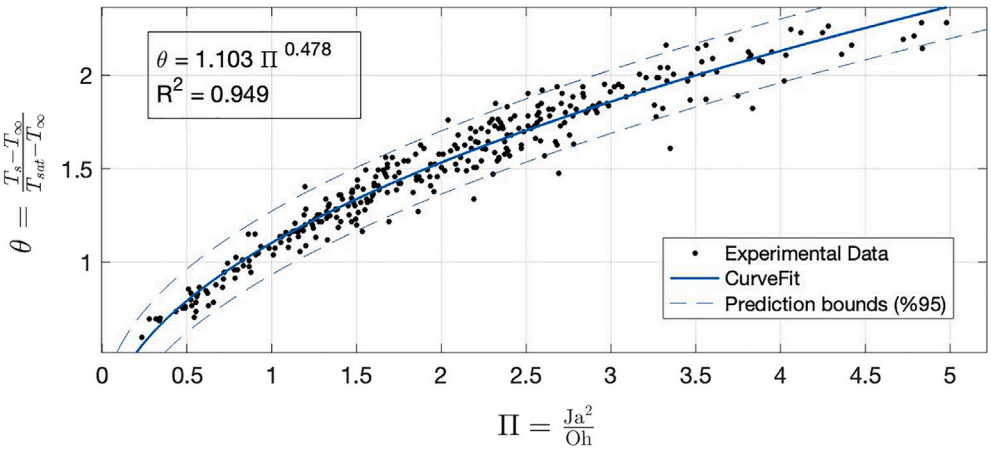

Fig. 8. Curve fit of nondimensional experimental data. The data for all three liquids are combined and shown.

Table 3
Summary of existing literature for modeling in film evaporation regime.

Authors	Droplet scale	Modeling information
Ebrahim et al. [6]	Single droplet (mm)	Analytical eq. for contact temperature
di Marzo and Evans [28]	Single droplet (mm)	Analytical eq. for heat flux
Huang et al. [29]	Single droplet (mm)	Analytical eq. for droplet temperature
Jaiswal and Khandekar [30]	Multiple droplet (mm)	Analytical eq. for heat transfer rate
Roisman [31]	Single droplets (mm)	Analytical eq. for contact temperature
Pasandideh-Fard et al. [13], Berberovic et al. [32] Strotos et al. [33], Guo et al. [34] Ruiz and Blake [35], Francois and Shyy [36] Chandra et al. [37], Teng et al. [38]	Single droplets (mm)	Numerical, Volume of Fluid (VOF)

3.2. Microdroplet lifetime on the surface

The microdroplet lifetime, or the resident time, on the surface is defined as the time interval between the impact moment until the microdroplet fully evaporates and vanishes. As mentioned previously in Section 1, only a few experimental studies on microdroplet impact exist. These studies mainly focus on unheated surfaces to explore the fluid dynamics, or in the Leidenfrost regime, or the impact of trains (consecutive) microdroplets [12,15,18,39,40]. To the best of our knowledge, there are no correlations to approximate the lifetime of a microdroplet on a heated surface. Predicting microdroplet lifetime at different impact conditions and surface temperatures can provide crucial information for the spray rate in spray cooling to avoid excessive liquid accumulation and reduction in heat transfer rate. In this research, the microdroplet lifetime was measured using the frame by frame analysis of high-speed videos in PCC software. The Leidenfrost regime was excluded as the microdroplet does not directly contact the surface. To properly normalize the lifetime, a time constant was derived by balancing the inflow of conduction heat and the absorbed heat by the droplet as follows

$$\frac{MC_p\Delta T}{\tilde{t}} \propto \frac{kA\Delta T}{D} \rightarrow \tilde{t} = \frac{D^2}{\alpha} \tag{5}$$

Fig. 9(a) shows the lifetime of a microdroplet on the surface for evaporation, boiling, and transition heat transfer regimes for all tested liquids. To capture the effect of all important parameters and involving dimensionless groups, the dimensionless lifetime, $\tau = \frac{t}{\tilde{t}} = \frac{t\alpha}{D^2}$, was multiplied by $\frac{1}{\Pi^2}$ where Π was previously defined as $\frac{Ja^2}{Oh}$. Nondimensional lifetime was curve fitted in MATLAB, as shown in Fig. 9(b), to develop a correlation to approximate how long it takes for a microdroplet to fully evaporate on a heated surface, given as

$$\frac{\tau}{\Pi^2} = \frac{t\alpha}{D^2}\frac{1}{\Pi^2} = 0.323\theta^{-8.656} + 0.123 \tag{6}$$

The ability to predict the lifetime of microdroplets can be integrated into and enhance spray cooling by pulsating the spray to avoid puddling, especially at lower surface temperatures where microdroplets take longer to evaporate. Furthermore, high-fidelity numerical simulations in boiling and transition regimes are challenging, thus, Eq. (6) and Fig. 9(a) provide accurate and valuable data for validation.

3.3. Evaporation time modeling for $T < T_{sat}$

Although the droplet heat transfer has been modeled analytically and numerically by numerous researchers, most of these studies focused on macrodroplets, critical heat flux, boiling, and the Leidenfrost regime. For example, modeling a droplet's contact duration with the surface in the Leidenfrost regime has been of particular interest [11,41–44]. Table 3 summarizes the existing literature for droplet heat transfer in the film evaporation regime ($T < T_{sat}$).

Since these models were derived for macroscopic droplets, the high advection field within the droplet caused by the significant flow field was considered in the derivation due to the spreading and receding phases. Ruiz and Blake [35] showed that the internal motion within the droplet provided an extremely different temperature field compared to the results of only considering conduction. The dimensionless analysis performed in Section 3.1 showed that the heat transfer of microdroplets was not affected by the impact velocity because the kinetic energy is negligible and therefore the heat transfer is diffusion dominant. As mentioned previously, the governing physics of a microdroplet

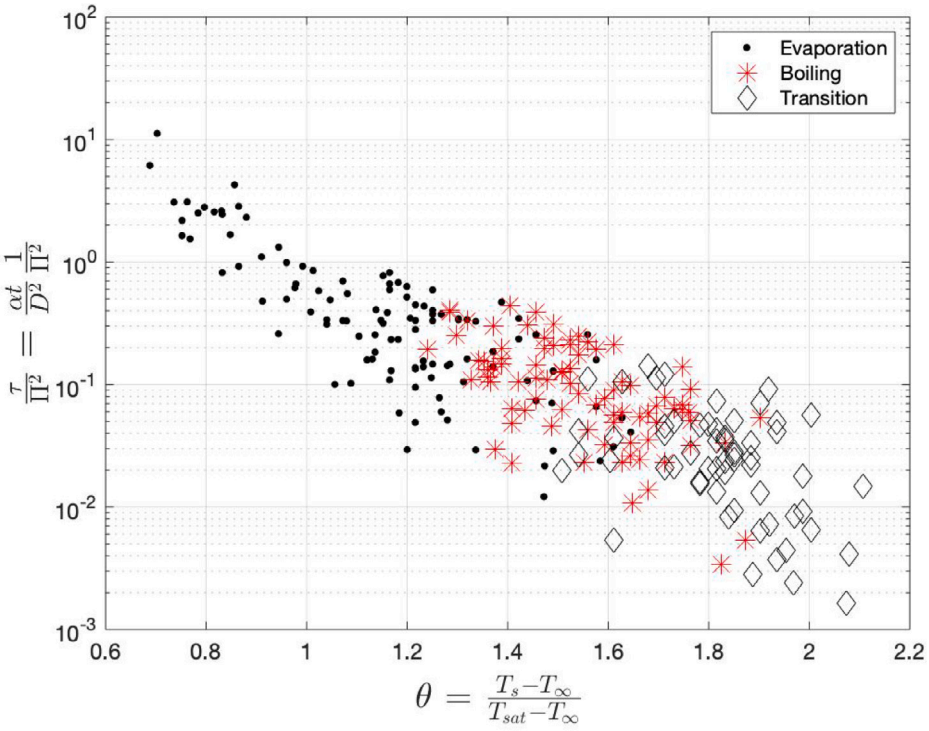

(a) Dimensionless lifetime vs. dimensionless surface temperature

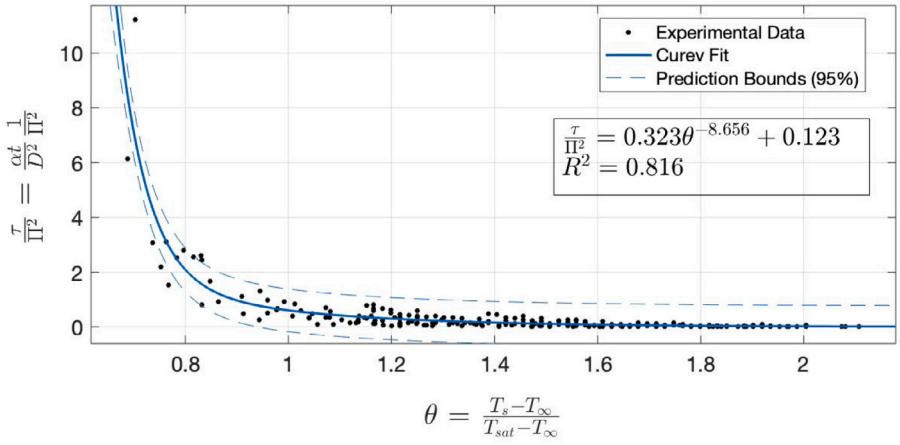

(b) Curve fit of dimensionless lifetime

Fig. 9. Microdroplet lifetime (duration of full evaporation) for all impact conditions of three liquids.

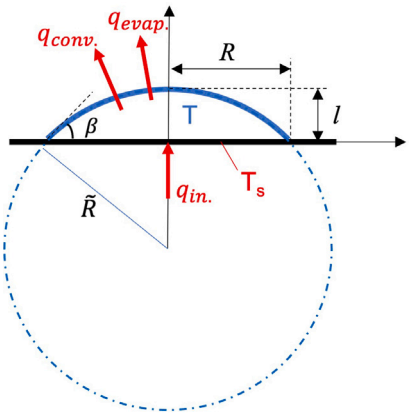

Fig. 10. Schematic of the assumed geometry of a microdroplet on a hot surface.

is fundamentally different from that of a macro-droplet, making the existing models inapplicable to microdroplets. Thus, none of the models in Table 3 can be applied to microdroplets.

In this paper, the conservation of mass and energy equations are solved for the evaporation rate of a microdroplet impacting a hot isothermal surface for $T < T_{sat}$. The energy balance for a control volume around a microdroplet shown in Fig. 10 can be written as

$$q_{in} - q_{evap.} - q_{conv.} = \frac{dE}{dt} = C_p \frac{d(mT)}{dt} \tag{7}$$

where T represents the droplet average temperature at the center, and $q_{in} = kA_c \frac{T_s - T}{\frac{l}{2}}$, $q_{conv.} = hA_s(T_s - T)$, and $q_{evap.} = \dot{m}_{evap.} h_{fg}$. A low heat transfer coefficient of $h = 10\ \frac{\mathrm{W}}{\mathrm{m}^2\ \mathrm{K}}$ was used as to model heat loss due to the free convection between the microdroplet surface and the ambient air. Since it was shown that the impact velocity effects are insignificant, the impact process is neglected in this model.

Substituting the heat flows into Eq. (7) and simplifying results in

$$kA_c \frac{T_s - T}{\frac{l}{2}} - hA_s(T_s - T) - \dot{m}_{evap.}(h_{fg} - C_p T) = mC_p \frac{dT}{dt} \tag{8}$$

where $m(t) = -\int \dot{m}_{evap.} dt$, derived from the conservation of mass. A spherical cap is assumed for the initial geometry of the droplet upon the impact. The droplet initial volume and the initial contact angle, β, can be used to find the initial volume of the spherical cap and thus the contact radius, R, and droplet height, l, at $t = 0$ through solving a system of equations as follows

$$\begin{cases} R = \tilde{R}\cos(90-\beta) & \text{(a)} \\ l = \tilde{R}(1 - \sin(90-\beta)) & \text{(b)} \\ \frac{\pi D^3}{6} = \frac{1}{3}\pi\tilde{R}^3\left(2 - 3\sin(90-\beta) + \sin^3(90-\beta)\right) & \text{(c)} \end{cases} \tag{9}$$

The experimental data shows that the droplet contact area on the surface remains constant for the majority of the evaporation process. Thus, R is assumed to be constant, and for simplicity, a cylindrical shape is assumed to find the instantaneous droplet volume on the surface as $\pi R^2 l(t)$, leading to $l(t) = \frac{m(t)/\rho}{\pi R^2}$.

The mass diffusion equation in the radial direction, given in Eq. (10), is solved to find the instantaneous $\dot{m}_{evap.}$.

$$\frac{1}{r^2}\frac{\partial}{\partial r}\left(D_{AB} r^2 \frac{\partial x_A}{\partial r}\right) = \frac{\partial x_A}{\partial t} \tag{10}$$

where D_{AB} is the mass diffusivity coefficient for liquid (A) and air (B), and x_A is the molar fraction of liquid vapor in air. The following initial and boundary conditions for Eq. (10) are given as

$$\begin{cases} x_A(r,0) = 0, & \text{(a)} \\ x_A(R,t) = \frac{P_{sat}}{P_\infty}, & \text{(b)} \\ x_A(\infty,0) = 0, & \text{(c)} \end{cases} \tag{11}$$

It is assumed that the air initially and at $r \to \infty$ contains no vapor of the liquid droplet. The molar flux of liquid (A) per unit area can then be found as $N(t) = -CD_{AB}\left(\frac{\partial x_A}{\partial r}\right)|_{(r=R)}$. Finally, the $\dot{m}_{evap.}$ is given as

$$\dot{m}_{evap.}(t) = MCD_{AB}A_s\left(\frac{\partial x_A(r,t)}{\partial r}\right)|_{r=R} \tag{12}$$

where M and C are the molar mass and the total concentration of the liquid, respectively.

Eq. (12) is coupled with Eq. (8) since $D_{AB} = f(T)$ and $A_s = f(l) = f(m)$. Thus, the system of differential equations were solved numerically to find the droplet's instantaneous temperature, $T(t)$, and mass, $m(t)$. Droplet lifetime can then be found when $m(t_{lifetime}) = 0$.

The experimental lifetime for an ethanol microdroplet is compared with the numerical data in Fig. 11 for a variety of impact conditions in the film evaporation regime. It can be seen that the proposed model can predict the evaporation time with a maximum error of 26.2%. Although this error may seem high, this model provides a straightforward approximation for the lifetime of a microdroplet under specific impact conditions for the first time. Also, this model confirms the characteristics of microdroplet heat transfer to be diffusion dominant. The lifetime data can be utilized in future studies to better control the spray rate and maximize the heat transfer while mitigating the excessive liquid accumulation on the surface.

4. Conclusions

The impact of single microscopic droplets of different liquids (ethanol, isobutanol, and isopropanol), generated by a piezoelectric dispenser, were studied on a heated surface $0.1 \le \mathrm{We} \le 6.5$ and $2 \le \mathrm{Re} \le 75$. The impact conditions of diameter, velocity, and temperature were varied to observe the dynamics of the impact for a broad range of variables. Four distinct heat transfer regimes of film evaporation, boiling, transition, and film boiling (Leidenfrost) were identified. A comprehensive and appropriately scaled phase diagram was developed to predict the heat transfer regime of a microdroplet for a given impact condition. It was shown that the initial kinetic energy had no effect on the impact dynamics. Correlations were developed to approximate the impact conditions required to achieve a certain heat transfer regime and to find the lifetime on the surface. The evaporation time (lifetime) for $T < T_{sat}$ can be estimated by numerically solving the proposed model derived from conservation laws. These results provide fundamental knowledge to better understand and control the spray cooling.

CRediT authorship contribution statement

Michael Hennessy: Writing – original draft, Visualization, Software, Project administration, Data curation. **Mahsa Ebrahim:** Writing – review & editing, Validation, Methodology, Investigation, Formal analysis, Conceptualization.

Declaration of competing interest

The authors declare that they have no known competing financial interests or personal relationships that could have appeared to influence the work reported in this paper.

Acknowledgments

We acknowledge the contributions of other undergraduate student research assistants Ashley Salisbury, Kennedy Necoechea, and David Kandah for collecting the experimental data.

Data availability

Data will be made available on request.

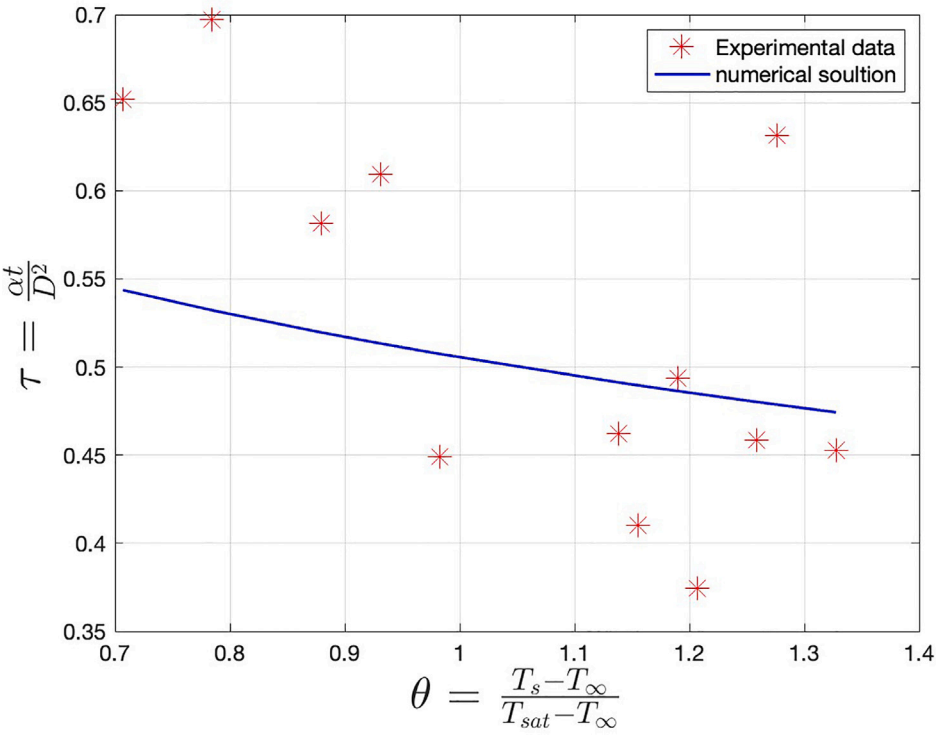

Fig. 11. Experimental lifetime of ethanol microdroplets compared with the numerical solution for the film evaporation regime ($\theta < 1.4$).

References

[1] G. Liang, I. Mudawar, Review of drop impact on heated walls, Int. J. Heat Mass Transfer 106 (2017) 103–126, http://dx.doi.org/10.1016/j.ijheatmasstransfer.2016.10.031, URL https://www.sciencedirect.com/science/article/pii/S0017931016324097.

[2] J. Breitenbach, I.V. Roisman, C. Tropea, From drop impact physics to spray cooling models: a critical review, Exp. Fluids 59 (3) (2018) 55.

[3] A. Yarin, Drop impact dynamics: Splashing, spreading, receding, bouncing, Annu. Rev. Fluid Mech. 38 (2006) 159–192, http://dx.doi.org/10.1146/annurev.fluid.38.050304.092144, URL https://www.annualreviews.org/content/journals/10.1146/annurev.fluid.38.050304.092144.

[4] T. Tran, H.J.J. Staat, A. Prosperetti, C. Sun, D. Lohse, Drop impact on superheated surfaces, Phys. Rev. Lett. 108 (2012) 036101, http://dx.doi.org/10.1103/PhysRevLett.108.036101, URL https://link.aps.org/doi/10.1103/PhysRevLett.108.036101.

[5] M. Ebrahim, A. Ortega, Identification of the impact regimes of a liquid droplet propelled by a gas stream impinging onto a dry surface at moderate to high Weber number, Exp. Therm. Fluid Sci. 80 (2017) 168–180, http://dx.doi.org/10.1016/j.expthermflusci.2016.08.019, URL http://www.sciencedirect.com/science/article/pii/S0894177716302242.

[6] M. Ebrahim, B. Elkenani, A. Ortega, Transient surface temperatures upon the impact of a single droplet onto a heated surface in the film evaporation regime, Int. J. Heat Mass Transfer 186 (2022) 122463.

[7] H. Nair, H.J. Staat, T. Tran, A. van Houselt, A. Prosperetti, D. Lohse, C. Sun, The leidenfrost temperature increase for impacting droplets on carbon-nanofiber surfaces, Soft Matter 10 (13) (2014) 2102–2109.

[8] M. Shirota, M.A. van Limbeek, C. Sun, A. Prosperetti, D. Lohse, Dynamic leidenfrost effect: relevant time and length scales, Phys. Rev. Lett. 116 (6) (2016) 064501.

[9] M. Ebrahim, A. Ortega, N. Delbosc, M.C.T. Wilson, J.L. Summers, Simulation of the spreading of a gas-propelled micro-droplet upon impact on a dry surface using a lattice-Boltzmann approach, Phys. Fluids 29 (7) (2017) 072104, http://dx.doi.org/10.1063/1.4989546, arXiv:https://doi.org/10.1063/1.4989546.

[10] G. Castanet, O. Caballina, F. Lemoine, Drop spreading at the impact in the leidenfrost boiling, Phys. Fluids 27 (6) (2015) 063302.

[11] G. Liang, S. Shen, Y. Guo, J. Zhang, Boiling from liquid drops impact on a heated wall, Int. J. Heat Mass Transfer 100 (2016) 48–57.

[12] C.W. Visser, Y. Tagawa, C. Sun, D. Lohse, Microdroplet impact at very high velocity, Soft Matter 8 (41) (2012) 10732–10737.

[13] M. Pasandideh-Fard, S. Aziz, S. Chandra, J. Mostaghimi, Cooling effectiveness of a water drop impinging on a hot surface, Int. J. Heat Fluid Flow 22 (2) (2001) 201–210.

[14] Y. Ko, S. Chung, An experiment on the breakup of impinging droplets on a hot surface, Exp. Fluids 21 (2) (1996) 118–123.

[15] H.-Y. Kim, S.-Y. Park, K. Min, Imaging the high-speed impact of microdrop on solid surface, Rev. Sci. Instrum. 74 (11) (2003) 4930–4937.

[16] A. Hu, D. Liu, 3D simulation of micro droplet impact on the structured superhydrophobic surface, Int. J. Multiph. Flow 147 (2022) 103887, http://dx.doi.org/10.1016/j.ijmultiphaseflow.2021.103887, URL https://www.sciencedirect.com/science/article/pii/S0301932221003001.

[17] A.-L. Zhang, J.-S. Zhang, X.-T. Fu, Y. Zha, Heating microdroplets on a piezoelectric substrate using intermittent surface acoustic wave, Ferroelectrics 486 (1) (2015) 41–48.

[18] G.E. Soriano, T. Zhang, J.L. Alvarado, Study of the effects of single and multiple periodic droplet impingements on liquid film heat transfer, Int. J. Heat Mass Transfer 77 (2014) 449–463.

[19] P. Dunand, G. Castanet, M. Gradeck, F. Lemoine, D. Maillet, Heat transfer of droplets impinging onto a wall above the leidenfrost temperature, Comptes Rendus Mécanique 341 (1–2) (2013) 75–87.

[20] S.M. Sellers, W.Z. Black, Boiling Heat Transfer Rates for Small Precisely Placed Water Droplets on a Heated Horizontal Plate, J. Heat Transf. 130 (5) (2008) 054504.

[21] F.-C. Chou, S.-C. Gong, C.-R. Chung, M.-W. Wang, C.-Y. Chang, Cooling of microspot by microdroplets, Japan. J. Appl. Phys. 43 (8R) (2004) 5609.

[22] H. Ulmke, T. Wriedt, K. Bauckhage, Piezoelectric droplet generator for the calibration of particle-sizing instruments, Chem. Eng. Technol.: Ind. Chemistry-Plant Equipment- Process. Engineering- Biotechnol. 24 (3) (2001) 265–268.

[23] H.J. Staat, T. Tran, B. Geerdink, G. Riboux, C. Sun, J.M. Gordillo, D. Lohse, Phase diagram for droplet impact on superheated surfaces, J. Fluid Mech. 779 (2015).

[24] J.D. Bernardin, C.J. Stebbins, I. Mudawar, Mapping of impact and heat transfer regimes of water drops impinging on a polished surface, Int. J. Heat Mass Transfer 40 (2) (1997) 247–267.

[25] V. Bertola, An impact regime map for water drops impacting on heated surfaces, Int. J. Heat Mass Transfer 85 (2015) 430–437.

[26] M. Khavari, C. Sun, D. Lohse, T. Tran, Fingering patterns during droplet impact on heated surfaces, Soft Matter 11 (17) (2015) 3298–3303.

[27] I. Roisman, J. Breitenbach, C. Tropea, Thermal atomisation of a liquid drop after impact onto a hot substrate, J. Fluid Mech. 842 (2018) 87–101.

[28] M. diMarzo, D.D. Evans, Evaporation of a water droplet deposited on a hot high thermal conductivity surface, J. Heat Transf. (Transcations the ASME (Am. Soc. Mech. Engineers), Ser. C);(USA) 111 (1) (1989).

[29] W. Huang, X. He, C. Liu, X. Li, Y. Liu, C.P. Collier, B.R. Srijanto, J. Liu, J. Cheng, Droplet evaporation on hot micro-structured superhydrophobic surfaces: analysis of evaporation from droplet cap and base surfaces, Int. J. Heat Mass Transfer 185 (2022) 122314.

[30] A.K. Jaiswal, S. Khandekar, Transient heat transfer during consecutive impact of two droplets on a heated substrate, Int. J. Therm. Sci. 193 (2023) 108546.
[31] I.V. Roisman, Fast forced liquid film spreading on a substrate: flow, heat transfer and phase transition, J. Fluid Mech. 656 (2010) 189–204.
[32] E. Berberovic, I.V. Roisman, S. Jakirlić, C. Tropea, Inertia dominated flow and heat transfer in liquid drop spreading on a hot substrate, Int. J. Heat Fluid Flow 32 (4) (2011) 785–795.
[33] G. Strotos, M. Gavaises, A. Theodorakakos, G. Bergeles, Numerical investigation on the evaporation of droplets depositing on heated surfaces at low Weber numbers, Int. J. Heat Mass Transfer 51 (7–8) (2008) 1516–1529.
[34] Y. Guo, S. Shen, S. Quan, Numerical simulation of dynamics of droplet impact on heated flat solid surface, Int. J. Low- Carbon Technol. 8 (2) (2012) 134–139.
[35] O.E. Ruiz, W.Z. Black, Evaporation of water droplets placed on a heated horizontal surface, J. Heat Transf. 124 (5) (2002) 854–863.
[36] M. Francois, W. Shyy, Part b: Fundamentals: Computations of drop dynamics with the immersed boundary method, part 2: Drop impact and heat transfer, Numer. Heat Transfer 44 (2) (2003) 119–143.
[37] S. Chandra, M. Di Marzo, Y. Qiao, P. Tartarini, Effect of liquid-solid contact angle on droplet evaporation, Fire Saf. J. 27 (2) (1996) 141–158.
[38] L. Teng, W. Wang, X. Huang, X. Luo, W. Li, J. Li, P. Yin, Y. Luo, L. Jiang, Evaporation of sessile droplet on surfaces with various wettability, Chem. Eng. Sci. 268 (2023) 118413.
[39] J. Breitenbach, I.V. Roisman, C. Tropea, Heat transfer in the film boiling regime: Single drop impact and spray cooling, Int. J. Heat Mass Transfer 110 (2017) 34–42.
[40] K.H. Al-Ghaithi, O.G. Harlen, N. Kapur, M.C. Wilson, Morphologies and dynamics of micro-droplet impact onto an idealised scratch, J. Fluid Mech. 925 (2021) A23.
[41] N. Hatta, H. Fujimoto, K. Kinoshita, H. Takuda, Experimental study of deformation mechanism of a water droplet impinging on hot metallic surfaces above the leidenfrost temperature, 1997.
[42] R.-H. Chen, S.-L. Chiu, T.-H. Lin, Resident time of a compound drop impinging on a hot surface, Appl. Therm. Eng. 27 (11–12) (2007) 2079–2085.
[43] A.-L. Biance, F. Chevy, C. Clanet, G. Lagubeau, D. Quéré, On the elasticity of an inertial liquid shock, J. Fluid Mech. 554 (2006) 47–66.
[44] R.-H. Chen, S.-L. Chiu, T.-H. Lin, On the collision behaviors of a diesel drop impinging on a hot surface, Exp. Therm. Fluid Sci. 32 (2) (2007) 587–595.